Preprint of:
Feng-Chuan F. Tsai, Novak S. Petrovic, Aleksandar D. Rakic
"Comparison of Stray-Light and Diffraction-Caused Crosstalk in Free-Space Optical Interconnects"
Proc. SPIE 5277, 320-327 (2004)

Comparison of Stray-Light and Diffraction-Caused Crosstalk in Free-Space Optical Interconnects

Feng-Chuan F. Tsai, Novak S. Petrović, Aleksandar D. Rakić
School of Information Technology and Electrical Engineering, The University of Queensland, Brisbane QLD 4072, Australia

ABSTRACT

In this paper we investigate for the first time the effect of the crosstalk introduced due to laser beam imaging in a free-space optical interconnect (FSOI) system. Due to the overfill of the transmitter microlens array by the vertical cavity surface emitting laser (VCSEL) beam, one part of the signal is imaged by the adjacent microlens to another channel, possibly far from the intended one. Even though this causes increase in interchannel and intersymbol interference, to our knowledge this issue has been neglected so far. The numerical simulation has been performed using a combination of exact ray tracing and the beam propagation methods. The results show that some characteristics of stray-light crosstalk are similar to that of diffraction-caused crosstalk, where it is strongly dependent on the fill factor of the microlens, array pitch, and the channel density of the system. Despite the similarities, the stray-light crosstalk does not affect by an increase in the interconnection distance. As simulation models for optical crosstalk are numerically intensive, we propose here a crosstalk behavioural model as a useful tool for optimisation and design of FSOIs. We show that this simple model compares favourably with the numerical simulation models.

Keywords: Stray light crosstalk, free space optical interconnect, diffraction

1. INTRODUCTION

Free-space optical interconnects (FSOIs) have been proposed as the solution to solve the limitation in electrical interconnect and the high demand in performance of short distance digital communication links [1-4]. FSOIs provide advantage in terms of low power consumption, wide bandwidth, fast speed and high capacity. They can be implemented in chip-to-chip or module-to-module interconnection systems within computers, telecommunications or data-communication systems.

One of the major factors that determine the channel capacity and signal-to-noise ratio is the optical crosstalk noise within the system. Furthermore, as the microlens diameter decreases to compensate for higher interconnect capacity, the performance of each channel will start to be limited by diffraction. Many researches have looked into the area of diffraction-caused crosstalk, where it assumed that majority of the energy from the laser beam will pass through the first microlens and the small amount of beam not passing through the expected microlens is ignored [5-7]. In reality, although this small portion of the laser beam did not propagate through the expected microlens, it still travels through the first microlens array via neighbouring microlens. This introduces a different kind of crosstalk named in the paper, the stray-light crosstalk, which has the potential to contribute significantly to the overall crosstalk within the FSOI system. Moreover, to our knowledge, many have investigated greatly into the diffraction-caused crosstalk, but rarely mentioned the stray-light crosstalk.

In this paper, we investigate the behaviour of the stray-light crosstalk. Then some simulation results for stray-light crosstalk will be presented and it will be compared with the diffraction-caused crosstalk noise in the FSOI system. Finally, an overall crosstalk noise behavioural model will be derived for future calculation.

2. FSOI SIMULATION MODEL DESCRIPTION

2.1 Basic model description

The basic model used for the simulation is shown in Figure 1. Figure 1 (a) displays a schematic of a microchannel FSOI using two set of microlens array, the VCSEL array and the photodetector array. It is assumed that the VCSEL array is located at $z = 0$ and the first microlens array is situated $z = d_1$ away from the VCSEL array. Then the second microlens

array is at a distance of $z = d_2 + d_3$ away from the first microlens array. Finally to allow the model to be a symmetrical system, the photodetector array is positioned $z = d_1 = d_4$ away from the second microlens. The waist of the VCSEL beam is ω_0, the pitch of the system is Δ, and the diameter of the microlens is D. Fill factor β is defined as the ratio of the array pitch and microlens diameter: $\beta = \Delta/D$. In Figure 1(b), the structure of the transmitter (T_x) microlens array or the receiver (R_x) microlens array is presented and the parameter definition is the same as in Figure 1(a).

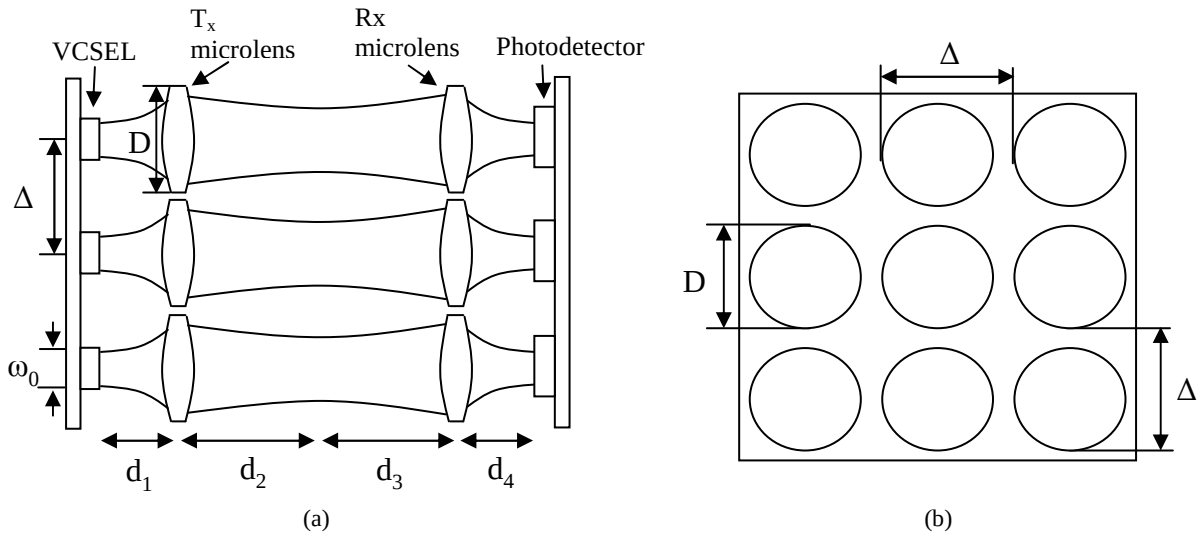

Figure 1: (a) Schematic of a microchannel free-space optical interconnect. (b) Structure of the T_x or R_x microlens array

2.2 Diffraction-caused crosstalk

A schematic of the FSOI model is shown in Figure 2. It can be assumed that a fundamental mode Gaussian beam is emitted from the VCSEL. Due to the diverging property of the Gaussian beam, the beam actually spreads as it reaches the transmitter microlens. The distance between the VCSEL and the transmitter microlens is set such that majority of the optical power is passed through the microlens. Once the beam travels through the microlens, it converges to its new beam waist, but when the new beam waist is reached, the beam will start to expand again. As the distance between the transmitter microlens and receiver microlens becomes greater, the beam will expand to a point where the beam radius is greater than the transmitter microlens aperture, then crosstalk will occur. This type of crosstalk will be referred as the diffraction-caused crosstalk [8] and it is shown in the region covered with black strip in Figure 2. It is also assumed that all the optical power that falls on the receiver microlens will be detected by its corresponding photodetector.

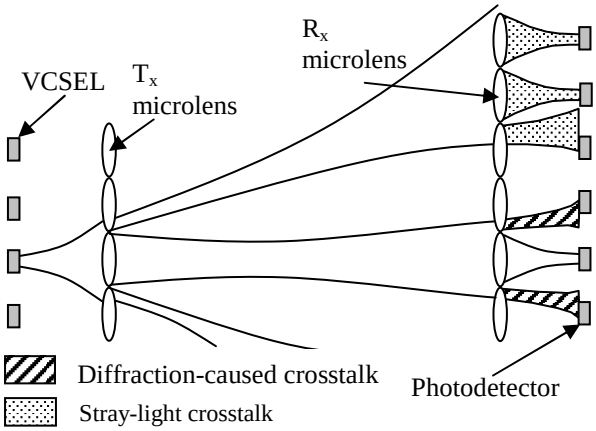

Figure 2: The schematic of free-space optical interconnect showing the diffraction-caused and stray light crosstalk

2.3 Stray-light crosstalk

Despite majority of the Gaussian beam propagating through centre channel transmitter microlens, a small portion of the beam will fall onto the neighbouring channel transmitter microlens. This is shown in Figure 2 and the small portion of the beam that fall onto the neighbouring channel transmitter microlens will be called the stray-light. The stray-light was then refracted away from the central channel because of the curvature of the neighbouring channel transmitter microlens. As it propagates through the system, the stray-light will expand more and more until it reaches the receiver microlens. Therefore as the interconnection distance increases, there will be more channels affected by the stray-light and hence creating stray-light crosstalk. This can be clearly seen in the dotted area of Figure 2.

With the idea of stray-light crosstalk noise produced from the centre channel in mind, it can be said that the total stray-light crosstalk noise from all other channels, which falls on the centre channel receiver microlens will be the same as the total stray-light crosstalk noise caused by the centre channel, because of the symmetrical nature of the microlens system. Consequently, the central surrounding channel will have much higher crosstalk noise than the channels near the boundary of the array.

3. SIMULATION RESULTS

The commercial simulation software Code V was used to simulate the stray light crosstalk. The stray-light crosstalk noise is measured by the amount of the encircled energy that falls on the receiver microlens plane of different channels. It is assumed that any encircled energy that fall on the receiver microlens will all be detected by the receiver. Throughout the simulation, the beam waist of 3 µm with a wavelength of 850 nm is used. The focal length of all microlens is 800 µm and the distance between the VCSEL and the transmitter microlens will be fixed at $d_1 = f + Z_R$, where f is the microlens focal length and Z_R is the Rayleigh Range. All the graphs presented in this section, the diffraction-caused and stray-light crosstalk noises are normalised to the power of the emitted beam.

3.1 Stray-light crosstalk characteristics

The normalised stray-light crosstalk noise with increasing system capacity for various values of fill factor, β is shown in figure 3. As the channels per mm^2 of the FSOI system increases, the stray-light crosstalk noise began to increase exponentially. Moreover, microlens with higher fill factor has greater increase in stray-light crosstalk noise as the array of channels of the system becomes larger. This indicates that stray-light crosstalk noise will increase considerably with a higher fill factor and greater system capacity.

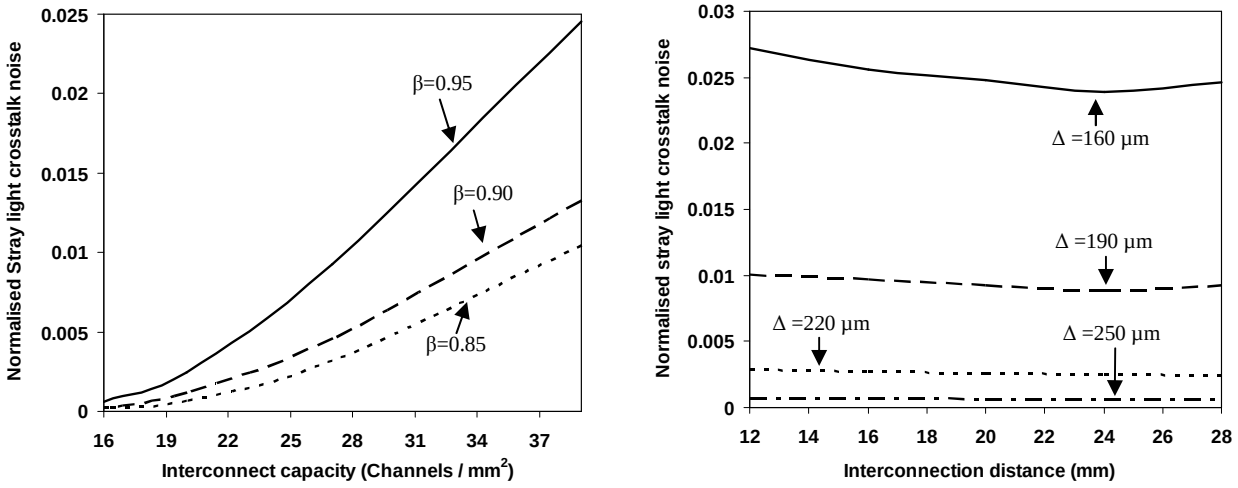

Figure 3: Stray-light crosstalk noise in both graphs is normalised to the power of the emitted beam. (a) Normalised Stray-light crosstalk noise with increasing system capacity (channels per mm^2) for various values of fill factor. (b) Normalised Stray-light crosstalk noise with increasing interconnection distance for various values of pitches

Figure 3 displays the normalised stray-light crosstalk noise with increasing interconnection distance for various values of pitches, Δ. The stray-light crosstalk noise only differs slightly as the interconnection distance increases. It is also evident that similar property is experienced for all other pitches. The only difference is that larger pitch will result in a lower stray-light crosstalk noise. This suggests that the stray-light crosstalk noise will not change noticeably with increasing interconnection distance.

3.2 Diffraction-caused and stray-light crosstalk comparison

The comparison between the normalised diffraction-caused and stray-light crosstalk with increasing system capacity for difference value of fill factor, β is shown in Figure 4. The figure suggests that the diffraction-caused crosstalk have similar characteristic as the stray-light crosstalk, as the system capacity increases the line start to increase exponentially. It is also evident that for both diffraction-caused and stray-light crosstalk, the slope of the graph is steeper with higher fill factor.

Figure 5 displays the comparison between the normalised diffraction-caused and stray-light crosstalk with increasing interconnection distance for different values of pitches, Δ. The graph shows that the characteristic of diffraction-caused crosstalk differs from stray-light crosstalk when the interconnection distance is increased. As the interconnection distance increases, the diffraction-caused crosstalk increase exponentially. Another characteristic should be noted is when the pitch is 250 μm, the diffraction-caused crosstalk will be more dominant when the interconnection distance is above 3 mm. Furthermore, when the pitch is reduced to 160 μm, the stray-light crosstalk will be more dominant till the interconnection distance is above 4.5 mm.

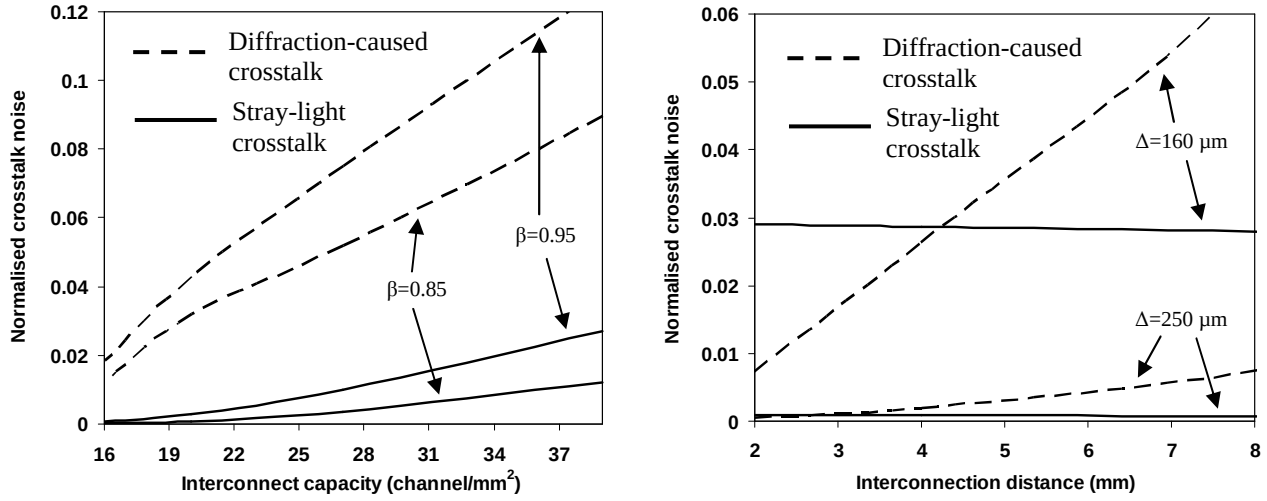

Figure 4: Diffraction-caused and stray-light crosstalk noise in both graphs is normalised to the power of the emitted beam. (a) Comparison of normalised diffraction-caused and stray-light crosstalk noise with increasing system capacity (channels per mm^2) for various values of fill factor. (b) Comparison of normalised diffraction-caused and stray-light crosstalk noise with increasing interconnection distance for various values of pitches

4. BEHAVIOURAL MODEL

During the simulation process, it is found that the simulation models for optical crosstalk are numerically intensive and also not everyone can obtain simulation software capable of calculating such models. For that reason, a behavioural model will now be proposed, which will become a useful tool for optimisation and design of FSOIs in the future.

4.1 Behavioural model formulation

Let the TEM_{nm} VCSEL beams be represented by Laguerre-Gaussian orthonormal functions:

$$\psi_{nm}(r,\theta,z) = K_{nm}\left(\frac{r\sqrt{2}}{w}\right)^{m} L_n^{(m)}\left(\frac{2r^2}{w^2}\right)\exp\left(\frac{-r^2}{w^2} - j\frac{kr^2}{2R}\right)\cos(m\theta) \tag{1}$$

where

$$K_{nm} = A_{nm}P_{nm} \tag{2}$$

and

$$A_{nm} = \exp\left\{ j\left[(2n+m+1)\arctan\frac{\lambda(z-z_s)}{\pi w_s{}^2} - k(z-z_s)\right]\right\} \tag{3}$$

and

$$P_{nm} = \frac{2}{w\sqrt{\pi(1+\delta_{om})}}\left[\frac{n!}{(n+m)!}\right]^{1/2}. \tag{4}$$

In the above equations, k is given as $k = 2\pi\lambda^{-1}$, and the Rayleigh range is given as $z_R = 0.5\, k\, w_s{}^2$. Beam waist, located at $z = z_s = 0$, is denoted by w_s.Beam radius at any distance z along the propagation axis is given as

$$w(z) = w_s\sqrt{1+\left(\frac{z}{z_R}\right)^2} \tag{5}$$

while the radius of curvature is given as

$$R(z) = z\left[1+\left(\frac{z_R}{z}\right)^2\right]. \tag{6}$$

The stray-light crosstalk noise will be calculated at the position of the transmitter microlens plane, located at $z = z_s + d_1 = d_1$, as shown in Fig. 1. The stray-light crosstalk noise is calculated as the portion of the light emitted by the central VCSEL that ends up on the immediately surrounding microlenses:

$$N = \int_A \left|\psi_{nm}(r,\theta,z_0)\right|^2 r\,dr\,d\theta. \tag{7}$$

In Eq. (7) A represents the area of the eight surrounding microlenses, $A = A_1 + A_2 + \ldots + A_8$, and z_0 indicated that integration is to be done at the transmitter microlens plane. Equation (7), as written above, can only be evaluated numerically, due to the fact that the total area A is composed of eight disjointed circles. In order to simplify the resulting model, at the cost of overestimating the stray-light crosstalk noise slightly, we can assume that A is equivalent to the area of the annulus A' shown in Figure 5.

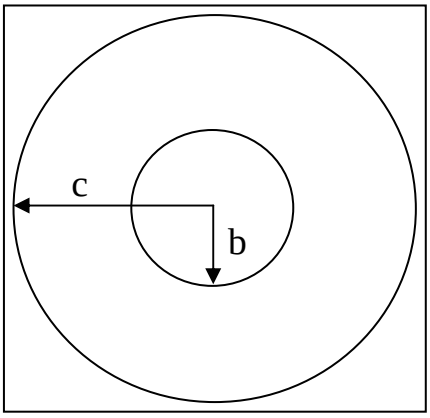

Figure 5: Schematic diagram of annulus *A*', the area of which is equivalent to *A*.

By evaluating Eq. (7) over *A*', the stray-light crosstalk noise due to any TEM_{nm} Laguerre-Gaussian beam is given as:

$$N = 2^{2-2n}\left(\frac{\sqrt{2}}{w_0}\right)^{2m}\sum_{p=0}^{n}\sum_{q=0}^{2p}\binom{2n-2p}{n-p}\binom{2p+2m}{2p-q}\frac{(2p)!}{p!q!}\left(\frac{1}{w_0}\right)^{2q}\frac{2^{q-m-2}}{(m+p)!}$$
$$\left\{b^{2m+2q}\left(\frac{b^2}{{w_0}^2}\right)^{-m-q}\Gamma\left(1+m+q,\frac{2b^2}{{w_0}^2}\right)\right. \tag{8}$$
$$\left.-c^{2m+2q}\left(\frac{c^2}{{w_0}^2}\right)^{-m-q}\Gamma\left(1+m+q,\frac{2c^2}{{w_0}^2}\right)\right\}$$

Given that the incident beam is the fundamental Gaussian TEM_{00} mode, Eq. (8) simplifies to

$$N = N_{00} = \frac{\Gamma(1,2{\kappa_1}^2)-\Gamma(1,2{\kappa_2}^2)}{{w_0}^2} = \frac{e^{-2{\kappa_1}^2}-e^{-2{\kappa_2}^2}}{{w_0}^2} \tag{9}$$

where

$$\kappa_1 = \frac{b}{w_0} \text{ and } \kappa_2 = \frac{c}{w_0} \tag{10}$$

and $w_0 = w(z_0)$, as given by Eq. (5), represents beam radius at the transmitter microlens plane. Annulus radii *b* and *c* are given as:

$$b = \Delta - \frac{D}{2} \text{ and } c = \sqrt{2}\Delta + \frac{D}{2}$$

Not all of the stray-light crosstalk noise that is introduced at the transmitter microlens will be detected by the photodetectors. The probability that N_{00} will fall on a microlens in the receiver microlens plane is equivalent to the ratio

of the area occupied by microlenses to the total area of the microlens array. Assuming that the array is infinitely big, the crosstalk noise will be given as

$$N_{SL} = \left(\frac{e^{-2\kappa_1^2} - e^{-2\kappa_2^2}}{w_0^2} \right) \left(\lim_{q \to \infty} \frac{\left(q^2 - 1\right)\left[\left(\frac{\beta\Delta}{2} \right)^2 \pi \right]}{(q\Delta)^2} \right) = \left(\frac{e^{-2\kappa_1^2} - e^{-2\kappa_2^2}}{w_0^2} \right) \left(\frac{\pi\beta^2}{4} \right) \tag{11}$$

where q denotes the number of channels in the microlens array. The probability coefficient $\eta = 0.25 \cdot \pi \cdot \beta^2$ was worked out with the implicit assumption that the stray-light crosstalk noise resembles a plane wave, i. e. that the beam intensity is the same regardless of the distance from the propagation axis. Since we assumed that the intensity of the emitted VCSEL beam has a Gaussian profile, we have to add a weighting coefficient to the probability coefficient, in order to account for the non-uniform intensity distribution at the receive microlens plane. The final expression for the stray-light crosstalk noise is

$$N_{SL} = \left(\frac{e^{-2\kappa_1^2} - e^{-2\kappa_2^2}}{w_0^2} \right) \left(\frac{\pi\beta^2}{4} \right)^t \tag{12}$$

where *t* is approximately 0.75.

4.2 Calculated and simulated model comparison

In Figure 6 (a), the simulated and calculated stray-light crosstalk noise is normalised to the power of the emitted beam. The figure shows the comparison of the simulated and calculated result for stray-light crosstalk noise with increasing system capacity for various values of fill factor, β. It can be concluded that the equation derived above is quite a good approximation for the stray light crosstalk.

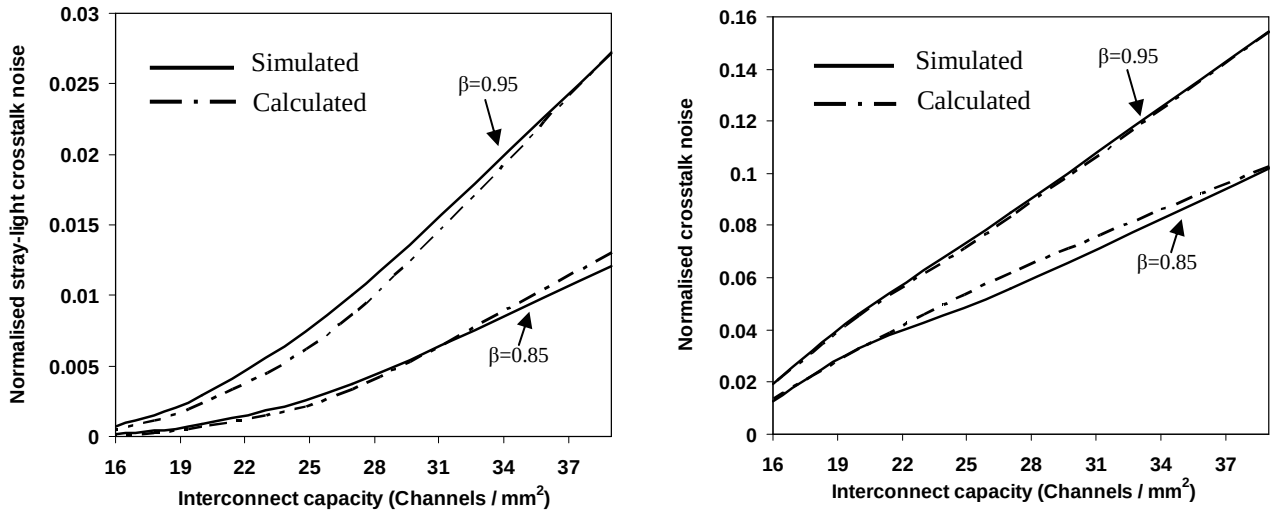

Figure 6: Simulated and calculated crosstalk noise in both graphs is normalised to the power of the emitted beam. (a) Comparison of simulated and calculated normalised Stray-light crosstalk noise with increasing system capacity (channels per mm^2) for various values of fill factor. (b) Comparison of simulated and calculated normalised crosstalk noise with increasing system capacity (channels per mm^2) for various values of fill factor.

Figure 6 (b) shows the simulated and calculated crosstalk noise, which is normalised to the power of the emitted beam with increasing system capacity for two different values of fill factor, β. Similarly to the previous figure, the calculated values matches well with the simulated values when the stray light crosstalk approximation is included into the overall crosstalk noise.

5. CONCLUSION

The characteristic of the stray-light crosstalk has been investigated for the first time to our knowledge. The numerical simulation has been performed using a combination of exact ray tracing and the beam propagation methods. The characteristics of stray-light crosstalk have been compared with that of the diffraction-caused crosstalk. It can be said that for both diffraction-caused and stray-light crosstalk are strongly dependent on the fill factor of the microlens, array pitch, and the channel density of the system. The only difference is when increasing in the interconnection distance, the diffraction-caused crosstalk will increase exponentially, but it has little influence on the stray-light crosstalk. As simulation models for optical crosstalk are numerically intensive, a behavioural model involving simple calculation has been proposed, which can be a useful tool for optimisation and design of FSOIs. The simple model compares favourably with the numerical simulation models. Furthermore it can be modelled by the simple equation and incorporated into the whole design for future calculation.

REFERENCES

1. D. A. B. Miller, “Invited paper: Physical reasons for optical interconnections,” International Journal of Optoelectron. Vol. 11, pp. 155-168, 1997.
2. R. Wong, A. D. Rakić, and M. L. Majewski, “Analysis of lensless free-space optical interconnects based on multi-transverse mode vertical-cavity-surface-emitting lasers,” Optics Communications, Vol. 167, pp. 261-271, August 1999.
3. D. A. B. Miller, “Rationale and challenges for optical interconnects to electronic chips,” Proceedings of IEEE, Vol. 88, pp. 728-749, 2000.
4. D. V. Plant, and A. G. Kirk, “Optical interconnects at the chip and board level: Challenges and solutions,” Proceedings of IEEE, Vol. 88, pp. 806-818, 2000.
5. E. M. Strzelecka, D. A. Louderback, B. J. Thibeault, G. B. Thompson, K. Bertilsson, and L. A. Coldren, “Parallel free-space optical interconnect based on arrays of vertical-cavity lasers and detectors with monolithic microlenses,” Applied Optics, Vol. 37, No. 14, pp. 2811-2821, May 1998.
6. X. Zheng, P.J. Marchand, D. Huang, O. Kibar, and S. C. Esener, “Cross talk and ghost talk in a microbeam free-space optical interconnect system with vertical-cavity surface-emitting lasers, microlenses, and metal-semiconductor-metal detectors,” Applied Optics, Vol. 39, No. 26, pp. 4834-4841, September 2000.
7. R. Wong, A. D. Rakić, and M. L. Majewski, “Design of microchannel free-space optical interconnects based on vertical-cavity surface-emitting laser arrays,” Applied Optics, Vol. 41, No. 17, pp. 3469-3478, June 2002.
8. N. S. Petrović, and A.D. Rakić, “Modeling diffraction in free-space optical interconnects by the mode expansion method,” Applied Optics, Vol. 42, No. 26, pp. 5308-5318, September 2003.